A METHODOLOGY FOR MORPHOLOGICAL AND CHEMICAL CHARACTERIZATION OF ASH DEPOSITS

Lucas Freitas Berti
Federal University of Santa Catarina, Department of Mechanical Engineering, Campus Trindade, Florianópolis, SC, Brazil 88040-900
berti@labcet.ufsc.br

Lourival Jorge Mendes Neto
Federal University of Santa Catarina, Department of Mechanical Engineering, Campus Trindade, Florianópolis, SC, Brazil 88040-900
mendes.lourival@gmail.com

Eduardo Gonçalves Reimbrecht
Federal University of Santa Catarina, Department of Mechanical Engineering, Campus Trindade, Florianópolis, SC, Brazil 88040-900
eduardo@labcet.ufsc.br

Edson Bazzo
Federal University of Santa Catarina, Department of Mechanical Engineering, Campus Trindade, Florianópolis, SC, Brazil 88040-900
ebazzo@emc.ufsc.br

Abstract. *Low ranking coal is currently used for steam generation in the Brazilian thermal power plants. A number of problems are associated to pulverized coal combustion, such as alkaline vapours, unburned char and ash particles deposition on the heat exchange surfaces. The deposits change the flow around the tubes and decrease the heat exchange. Besides the plugging and tube wastage by impact, the ash deposits imply in an operational problem involving non programmed stops of the boiler, increasing the operation and maintenance costs. This work concerns a new methodology for morphological and chemical characterization of ash deposits located on the boiler superheater and some bottom ashes from Jorge Lacerda thermal power plant. Concerning some important parameters on the deposition mechanisms, different techniques were used to characterize the existing ash deposits and the bottom ashes, such as helium pycnometry, image analysis and porosity determination based on the Archimedes' principle. The chemical compositions were determined by X-Ray Difratometry carried out in ash deposits, bottom ashes and coal samples.*

Keywords*: Morphological Characterization, Chemical Composition, Ash Deposit, Bottom Ash, Low Ranking Coal.*

1. INTRODUCTION

Thermal power plants supply approximately 20% of energy required in Brazil according to ANEEL (2007). Nowadays coal, as fuel, is responsible for approximately 9% of the thermal power plant. For the next years, it represents 29% of the futures thermal plants, ANEEL (2007). The use of coal has several important issues such as air pollution and water heating. After milling, the pulverized coal is injected into the boiler for burning, by this way producing the required heat for steam generation. Most of the coal used in the thermal power plant comes from the southeast region of Brazil, namely Santa Catarina state. This coal presents almost 40% of ash (Reinaldo, 2004 and Mendes *et al* 2005) in its composition which harms the availability of the system. One of the drawbacks of ash, presented in the coal, is the insulation of the heat exchange tubes by the ash deposit growing on the surfaces. As an immediate consequence of the deposition is the decrease of the boiler efficiency.

In order to analyze the heat transfer through the ash deposit it is necessary to characterize the morphology and the chemical composition of the porous structure. In this work it is presented a methodology to describe and to complement some previous work (Mendes *et al*, 2005). The methodology includes density, porosity, pore size distribution and self-correlation analysis of some sampled images taken from a typical ash deposit, also were determinated the chemical composition of the deposits.

The image analysis were evaluated by a image software Imago® developed by the Laboratory of Porous Media and Thermophysical Properties (LMPT/UFSC) as shown by Fernandes, 1994 and Philippi *et al*, 2000. The image analysis provides all the necessary data to the evaluation of morphologic properties of the ash deposit used here. All images were collected in Scanning Electron Microscope (SEM) available at the Microstructure Characterization Laboratory (LCM/UFSC). This technique was complemented by experimental methodologies, such as, Archimedes' principle and the helium pycnometer. The chemical composition was determined from the X-Ray Difratometry and energy dispersive X-ray analysis also available at LCM/UFSC.

2. MATERIALS AND METHODS

For the calculus of porosity, the Archimedes' principle was used. The methodology used followed the standard MPIF-42 (1997).

Another way to determine porosity is through digital images analysis. Digital images had been collected in a Philips Scanning Electron Microscope (SEM), Series XL-30. The SEM images were detected with backscattered electron with 100x magnification. Concerning the fragile nature of the samples, its preparation is a delicate task. All the cuts on the samples were made in the precision cutting, model ISOMET 1000 - Buehler, with distilled water to prevent any contamination.

Two cut directions were elected to analyze the morphologic characteristics of the sample, as shown in Fig.1. The "Direction 1" is perpendicular to the heat exchange tube and "Direction 2" is approximately the gas flow direction to the tube. All the samples were mounted in a special resin epoxy, Epofix®, in a vacuum chamber.

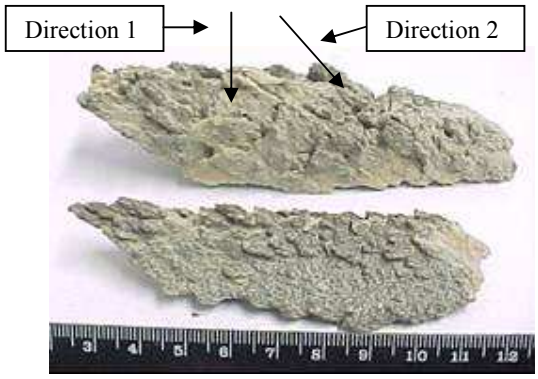

Figure 1 – Typical ash deposit from the boiler superheater

The samples were classified in two groups, according to the visual aspects:

-porous;
-dense;

and subdivided according to:

-superior part;
-inferior part.

All the samples have different visual aspects. The samples that look like more compact and rigid were labeled as dense. The samples that look like a more porous structure were labeled as porous. In addition, taking into account the influence of heat transfer through the deposit, the samples were analyzed considering two different parts. Then, the position of the sample closer to the tube is referenced as inferior part and the superior part is the position closer to the gas flow. The samples and the nomenclature are described on the Table 1.

Table 1. Samples nomenclature.

Sample	Visual aspect	Cut direction
1	Dense	1
2	Porous	1
3	Dense	1
4	Porous	1
5	Dense	2
6	Porous	2

All the images were analyzed through the use of Imago® software. This software uses digital images to determine the morphologic properties of the sample, such as porosity, pore size distribution and self-correlation.

To determine an average value of the sample properties, a number of **n** images have to be considered. After processing 20 images the porosity hasn't change its average value, so it were adopted that 20 images would be enough to represent the average properties of the sample.

The helium pycnometer were used for the density characterization, it is based on the Archimedes' principle of the fluid displacement and on the Boyle's law. The Miltipycnometer - Quanta Chrome was used and Helium 5.0® White Martins as the gas work. Before this procedure, the mass of samples were determined, with a precision balance, model Adventurer - Ohaus, with a 0.0001 g precision. This process allows determining the bulk density. All the samples were milled with 80 mesh.

The X-ray difratometry, XRD, utilizing an equipment X´Pert – Phillips, is an important tool of characterize of the crystal structure. The XRD is based on the oscillating behavior of X-Ray and its interaction with atoms of crystal

structure from the powdered sample. The parameters used for this analysis were: characteristic radiation of Cu Kα equal to 1.54056 nm and varying angle 2θ from 3º to 118º, using 0.05º as goniometric step motion. The operation tension is of 40kv with 30mA.

The proposed nomenclature for XRD analyzes is:

a) "Sample A", for the samples collected on heat exchange tubes;
b) "Sample B", for the samples collected on the bottom of the boiler;
c) "Sample C", for the coal used as fuel.

3. RESULTS AND DISCUSSION

The Table 2 shows the porosity obtained from experimental method based on Archimedes' principle. The porosity values observed on this test confirms the visual aspect division of the samples adopted on this work.

Table 2. The value of the sample porosity.

Sample	Porosity [%]
1	16,0
2	21,3

The digital analyses will be presented graphically. The self-correlation curves of the samples 1 to 6 are shown on the Figure 2 to Figure 4, respectively.

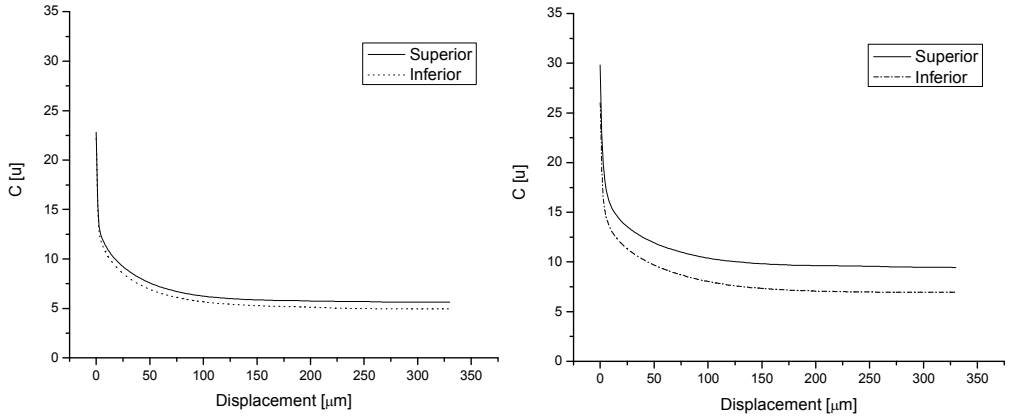

a b

Figure 2. Self-correlation curve of the samples 1 (a) and 2 (b)

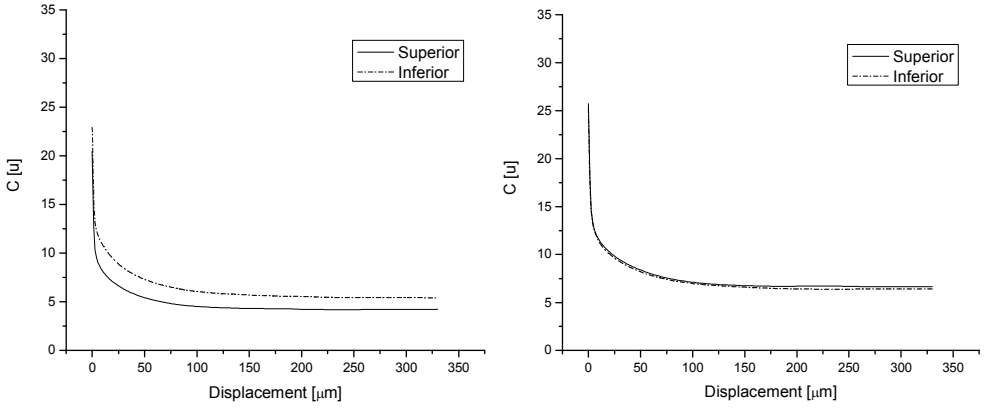

a b

Figure 3. Self-correlation curve of the samples 3 (a) and 4 (b)

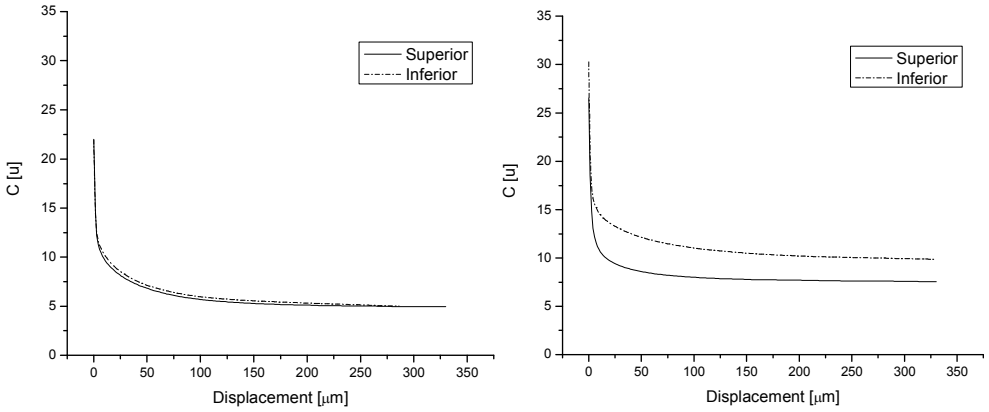

a b

Figure 4. Self-correlation curve of the samples 5 (a) and 6 (b)

The self-correlation represents the probability of two elementary cells separated by a displacement, u, belongs to the same structure, according to Fernandes and Philippi (1994). Besides, in order to the image represents the porous media it is necessary that the self-correlation curve must tend quickly for a characteristic value. Here, this behavior was not observed on all of the images analyzed. The self-correlation function of the superior part of the sample presented on Fig. 4 (b), amongst all, is the one that indicates a most correlated image on this magnification. Figure 5 shows a typical image, collected from the SEM, of the ash deposit and its binary image.

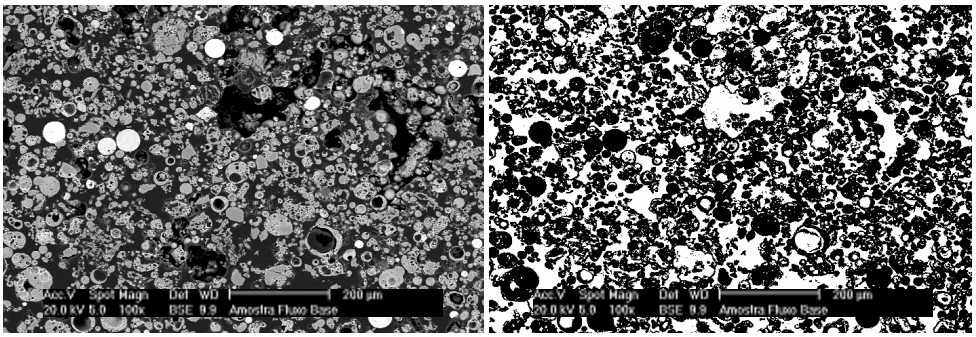

a b

Figure 5. Typical image from sample 6 (a) and its binary image (b)

In Fig.5 (a), the dark point represents void and the light points represent the ash particles. The Imago® considers, on the binary image, the white points for the calculus of the morphological properties. For that reason, the voids are represented by white points and the structure is represented by the black ones, as shown in Fig.5 (b). The resolution used here is the 100x magnification, which means that one pixel corresponds to 1.36 μm.

The pore size distributions of the samples 1 to 6 are shown in the Figure 6 to Figure 8, respectively.

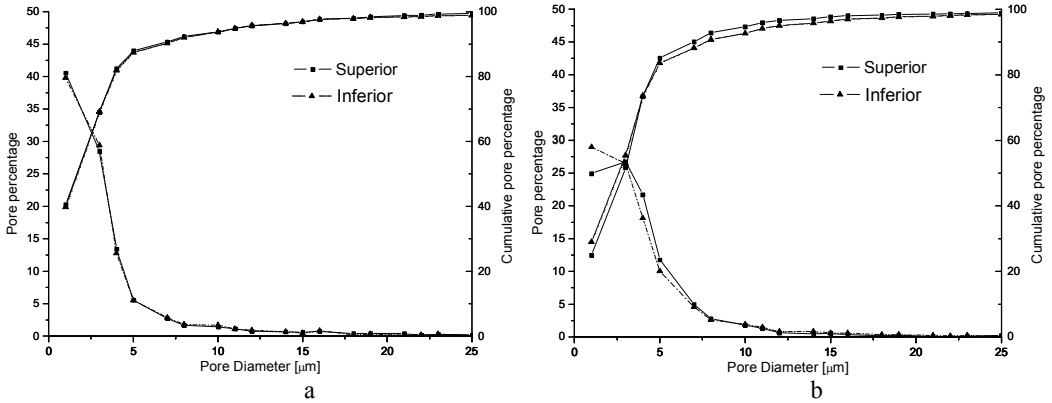

a b

Figure 6. Pore size distribution of the samples 1 (a) and 2 (b)

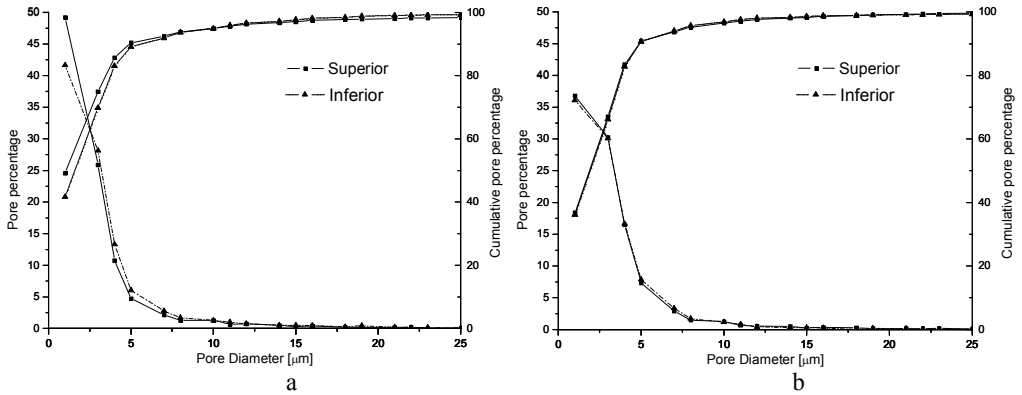

Figure 7. Pore size distribution of the samples 3 (a) and 4 (b)

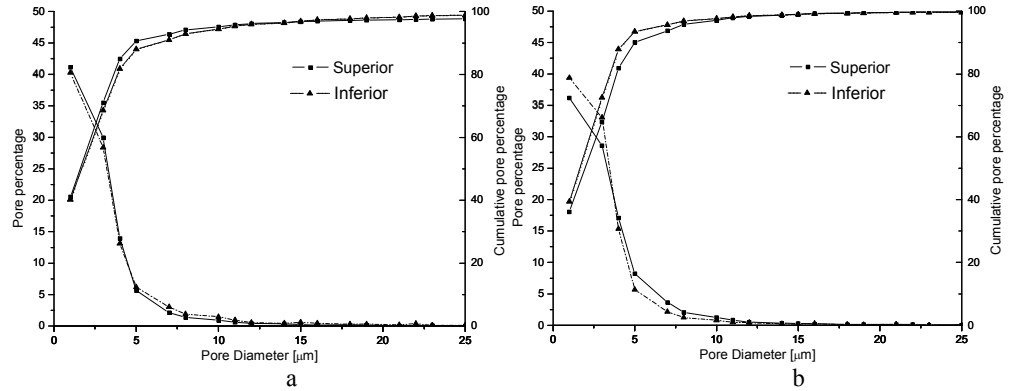

Figure 8. Pore size distribution curve of the samples 5 (a) and 6 (b)

From Table 3 it possible to verify that 90%, D_{90}, of pore size are, in average, smaller than 6 μm. The D_{90} of sample part "2 – inf" and "6 – inf" presented values different from the average, probably because the cut direction were made on a non-representative sample location. Table 3 shows the average porosity and D_{90} for the samples analyzed.

Table 3. Pore size distribution.

Sample - localization	Average Porosity [%] / Standard Deviation	D_{90} [μm]
1 – inf	22,2 / 0,6	6,8
1 – sup	22,8 / 1,1	6,8
2 – inf	26,0 / 1,1	8,2
2 – sup	29,8 / 1,4	6,8
3 – inf	22,9 / 1,6	5,4
3 – sup	20,5 / 0,4	5,4
4 – inf	25,2 / 0,8	5,4
4 – sup	25,7 / 0,6	5,4
5 – inf	22,0 / 0,7	6,8
5 – sup	21,9 / 0,7	5,4
6 – inf	30,3 / 2,0	4,1
6 – sup	26,5 / 1,5	5,4

On Table 3 it is possible to verify the difference between the porous and dense samples. This difference can also be verified on the Table 4 which shows the comparison between the techniques used for the porosity analyzes of the samples.

Table 4. Porosity comparison between techniques

Technique	Visual appearance	Direction	Average porosity [%]
MPIF-42	Porous	-*	21,3
MPIF-42	Dense	-*	16,0
Image analysis	Porous	1	26,7
Image analysis	Dense	1	22,1
Image analysis	Porous	2	28,4
Image analysis	Dense	2	22,0

* Not applicable to this classification

From the digital image analyses the porosity for Direction 1 and Direction 2 are almost the same, but for the Archimedes' principle technique it presented different value. This difference can be explained by an addition of closed porosity value which is not taking into account by the experimental technique.

Another technique used here is the helium pycnometry. This experimental technique was employed for particles density determination. The Table 5 shows the density of the groups.

Table 5. Average density of the particles of the samples.

Sample	Average density [g/cm^3]
Dense	3,229
Porous	3,230

From Table 5 can be verified that, in average, the particles of the ash deposit have the same density. With these values is possible to estimate an apparent density for the dense and porous group, which consists of multiplication of the solids fraction with the average density. The apparent density of the denser and porous groups is 2.71 g/cm^3 and 2.54 g/cm^3 respectively. For this estimation it was considered the porosity from experimental method the MPIF-42.

The chemical composition of ash deposit samples is shown in Table 6 and Table 7, for sample A and B, respectively.

Table 6. Chemical composition of sample A (Reinaldo, 2004).

Component	Quantity (%)
Silicon oxide (SiO_2)	28.02
Alumina (Al_2O_3)	16.63
Iron oxide (Fe_2O_3)	45.99
Potassium oxide (K_2O)	0.23
Calcium oxide (CaO)	2.82
Magnesium oxide(MgO)	0.41
Sodium Oxide (Na_2O)	0.77
L.O.I	3.17

Table 7. Chemical composition of sample B (Reinaldo, 2004).

Component	Quantity (%)
Silicon oxide (SiO_2)	57,04
Alumina (Al_2O_3)	26,55
Iron oxide (Fe_2O_3)	6,88
Potassium oxide (K_2O)	2,76
Calcium oxide (CaO)	2,10
Titanium oxide (TiO_2)	1,34
Magnesium oxide(MgO)	0,95
Sodium Oxide (Na_2O)	0,47
Phosphate (P_2O_5)	0,08

An ultimate and elementary chemical analysis was applied for the coal average composition, as presented in Table 8 and Table 9, respectively.

Table 8. Immediate analysis of sample C (Reinaldo, 2004).

Component	Quantity (%)
Volatile Material	20,9
Fixed Carbon	32,1
Inorganic Material	37,0
Humidity	10,0

Table 9. Elementary analysis of sample C (Reinaldo, 2004).

Component	Quantity (%)
Carbon	43,04
Hydrogen	2,87
Sulfur	2,87
Oxygen + nitrogen	4,22

Sample A presented a large amount of iron, silicon oxide and alumina on its chemical composition. This composition is presented in different phases, as show in Fig. 9. The Figure 9 presents the X-ray analysis of the samples A.

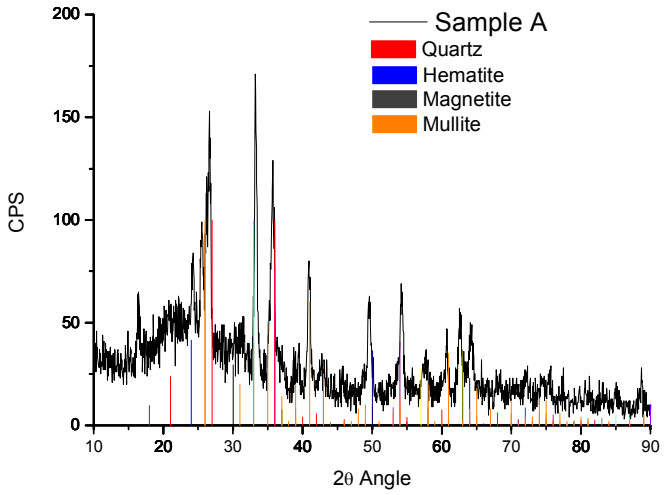

Figure 9. X-ray pattern of sample A

The sample A presents an amorphous phase evidenced by the lump between region of the angles 15º and 40º. Due to the high concentration of Silicon oxide, Iron Oxide and Aluminum oxide, sample A presents three phases with this chemical composition. These phases are Quartz, 862237 JCPDS (1981); Hematite, 850599 JCPDS (1981); Magnetite, 790418 JCPDS (1981), and Mullite, JCPDS 150776 (1981).The X-ray diffraction of sample B is shown on Fig.10.

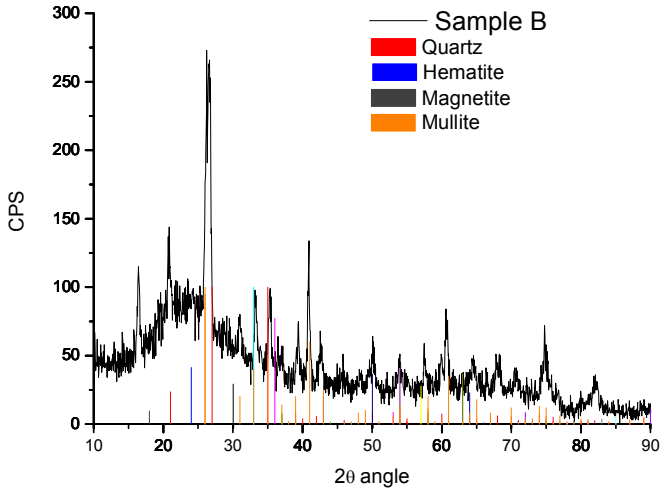

Figure 10. X-ray pattern of sample B

Mullite, Hematite, Magnetite and Quartz are also present on sample B as shown on Fig. 10. The presence of Mullite and Quartz phases on the samples are supported by the chemical composition shown on Table 7, especially because of the large amount of Silicon oxide and Aluminum oxide. The difference between the chemical composition of the samples A and B is mostly because of higher concentration of Silicon and Iron oxide, as the Mullite is mostly a result from the combustion process, it is expected that this higher concentration of Silicon oxide on the Sample B is due to the presence of high content of Quartz. Also the higher concentration of Iron oxide on the sample A, from the heat exchange tube, can be explained by an absorption mechanism of the Iron from the tube, wasting it, due to the high temperature gradient.

The sample C X-ray diffraction is shown on Fig.11.

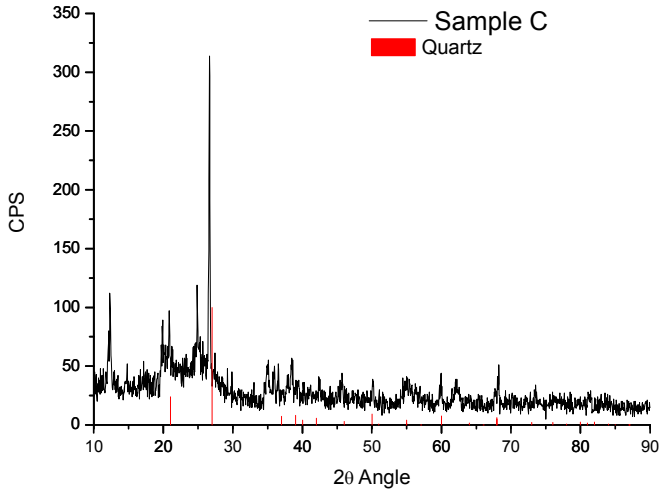

Figure 11. X-ray pattern of sample C

On Figure 11 can be verified the quartz phase presented on coal. This is the possible source for the quantity of quartz present on the ash deposits, as can be verified on the other samples. Mullite, Hematite and Magnetite are possible resulting phases from the coal combustion and fusion process on the ash deposit due to the heat transfer. This is supported by Figure 11 which does not have any presence of these phases.

3. CONCLUSION

The proposed methodology is a reliable tool for an effective morphological and chemical characterization of coal and boiler ash deposits. According to the found results, it was concluded:

a. The mean dense group porosity is smaller than the porous group porosity, respectively 16% and 21%, considering the experimental techniques, according to the visual aspect.
b. The mean dense group porosity is almost the same for both sample cut direction, around 22%;
c. The mean porous group porosity is almost the same for both sample cut direction, around 27%;
d. The difference between experimental and digital image analysis techniques can be explained by the existing close porosity in the samples.
e. All images did not present a good self-correlation curve, for the used 100x magnification;
f. Concerning the pore size distribution, the D_{90} of the samples are approximately 6 μm; there are no pores bigger than 20 μm;
g. The particles density is the same for both groups, around 3.23 g/cm^3;
h. The ash deposits presented a large amount of iron, silicon and aluminum oxide, which are the possible sources for hematite, magnetite, mullite and quartz phases found on the ash deposits;
i. The coal sample has a large amount of inorganic compounds, possibly the source of the found quartz phase on the ash deposit.

4. ACKNOWLEDGEMENTS

Thanks the Brazilian agency CNPq (Conselho Nacional de Desenvolvimento Científico e Tecnológico) for financial support. Special thanks are given to Tractebel Energy (project P&D ANEEL) and to Eng Luis Fellipe for allowing the access to the power plant. Also, thanks are given to Professor João Cardoso de Lima from Physics Department - UFSC, for the technical support on phase identification. Thanks to Laboratory of Porous Media and Thermophysical Properties (LMPT/UFSC) and ESSS Company for the software IMAGO® license.

5. REFERENCES

ANEEL, 2007. “Agência Nacional de Energia Eletrica”. 4th Apr. 2007, <http://www.aneel.gov.br/aplicacoes/capacidadebrasil/OperacaoCapacidadeBrasil.asp>

Fernandes, C. P; Philippi, P. C., 1994, “Caracterização morfotopologica de espaços porosos: reconstituição multiescala e simulação de processos de invasão de fluidos não-molhantes”. Doctoral Thesis, at Federal University of Santa Catarina.

MPIF Standard 42, 1997, “Determination of Compacted or Sintered Powder Metallurgy Products”, Metal Powder Industries Federation, issue 1980, revised 1986.

Mendes L.J.N., Figueiredo W., Bazzo, E., Azevedo J.L.T., 2005, “Boiler ash deposit characterization of Brazilian pulverized coal using scanning electronic microscopic”, In: Eighth International Conference on Technologies and Combustion for a Clean Environment, Proceedings of CLEAN AIR 2005 Lisbon.

Reinaldo, R. F.; 2004, “Estudo numérico da transferência de calor e deposição de cinzas em caldeiras com queima de carvão pulverizado”; Doctoral Thesis, at Federal University of Santa Catarina, Florianópolis.

Philippi, P. C; Damiani, M. C; Fernandes, C. P; Bueno, A. D.; Santos, L. O. E; Cunha Neto, J. A. B, 2000 “Characterization of reservoir rocks from image analysis on software imago”, Proceeding of the Workshop da Sub-rede Modelagem, Imagem e Visualização da Rede Recope/FINEP Aplicações da Informática à Engenharia, pp 32-36.

JCPDS (Power diffraction file search manual); International Centre for Diffraction Data: Pennsylvania, 1981.

6. RESPONSIBILITY NOTICE

The authors are the only responsible for the printed material included in this paper.